Acoustic Emission Feature Extraction and Classification for Rail Crack Monitoring

Conference Paper · November 2019

DOI: 10.12783/shm2019/32434

4 authors, including:

Dan Li
Southeast University (China)

Shaopeng Xu
Hunan University

Acoustic Emission Feature Extraction and Classification for Rail Crack Monitoring

DAN LI, SHAOPENG XU, YANG WANG and WEIXIN REN

ABSTRACT

Crack monitoring of rails aims to identify fatigue cracks in advance in order to ensure a safe and smooth operation of railway system. This study focuses on the rail crack monitoring using acoustic emission (AE) technique in the railway field typically with complex crack conditions and high operational noise. There are mainly three types of AE waves respectively induced by operational noise, crack propagation and impact, which need to be carefully distinguished from each other for the sake of quantitative crack monitoring. Wavelet transform (WT) was applied to represent the features of AE waves in the time-frequency domain. AE waves induced by different mechanisms were found to contain various instantaneous frequency components. A deep convolutional neural network (CNN) with transfer learning was proposed as an automatic feature extractor and classifier to evaluate the WT plots of AE waves. The CNN was trained, validated and tested using AE data collected through field and laboratory tests. The results demonstrated that the proposed methodology performed well in classifying AE waves induced by different mechanisms in the railway field.

INTRODUCTION

Rail defects due to dynamic wheel-rail interaction and harsh environmental exposure could result in operational downtime and catastrophic failures. Fatigue cracks are one primary type of rail defects, but more difficult to be detected than other types like corrugations and spallings [1]. Rail crack monitoring is able to identify fatigue cracks in time and helps to ensure a safe and smooth operation of railway system. Acoustic emission (AE) technique provides a promising approach for efficient rail crack monitoring. AE refers to the generation of transient stress waves during processes of cracks, fractures and impacts. AE waves contain valuable information related to the microstructural changes and therefore can be utilized to detect structural defects without any external ultrasonic inputs. Compared with other non-destructive testing (NDT) techniques [2], AE technique is more sensitive to crack initiation and

Dan Li, Shaopeng Xu, Yang Wang and Weixin Ren
School of Civil Engineering, Hefei University of Technology, Hefei, 230009, China

propagation, less influenced by the structural geometry, more capable of long-distance crack detection, and capable of detecting both surface and internal cracks [3]. A number of laboratory and field studies have been reported recently to detect and locate rail cracks using AE technique [4-7].

Multiple types of AE waves could be generated by different mechanisms in the railway field, such as operational noise, crack propagation and impact [6]. Operational noise is mainly introduced by the wheel-rail rolling contact and interaction. Crack propagation-induced AE waves are the primary events that happen during crack growth and can be used to detect both surface and internal cracks. Impact-induced AE waves occur when train wheels pass over a surface crack with unevenness or spalling. AE crack detection strategies for rolling bearings generally make use of the impact-induced AE waves, aiming at detecting surface defects of rolling elements [8,9]. AE waves corresponding to different mechanisms should be carefully distinguished from each other for the sake of accurate crack identification and quantitative crack evaluation. It is not an easy task because the raw AE measurement could be a complex combination of waves contributed by various mechanisms, the signal-to-noise ratio (SNR) of AE waves collected in the field rail are generally very low, and the amplitude and intensity of these AE waves could vary dramatically due to different crack conditions, train speeds and track types.

In order to conduct accurate classification of AE waves, it is meaningful to preprocess the data in an appropriate way. Wavelet transform (WT) is a powerful tool to represent the features of non-stationary signals like AE waves in the time-frequency domain. AE waves associated with different mechanisms are found to contain various instantaneous frequency components that can be observed in the WT plots [10]. Besides, WT is able to suppress the influence of noise by filtering out the corresponding frequency components or selecting characteristic frequency bands [6]. Indexes can be established based on WT coefficients to distinguish the mechanisms of AE waves [4,10]. Since a large amount of AE data would be collected in the field, it is difficult to develop a simple index to efficiently extract intrinsic features of the WT plots and to directly classify different types of AE waves induced by naturally formed rail cracks. Therefore, machine learning techniques have been introduced by taking the results of time-frequency analysis as the inputs [11,12].

In recent years, deep learning algorithms that are composed of multiple processing layers turn out to be very good at discovering intricate structures in large high-dimensional data sets [13]. Convolutional neural network (CNN), one particular type of feedforward neural network in deep learning field, has won numerous contests in pattern recognition. It is inspired by the visual cortex of animals, and is much easier to train and generalized much better than networks with full connectivity between adjacent layers. It is highlighted in automatic feature extraction and classification of images without any hand-crafted features [14,15]. This matches the goal to classify WT plots, which are two-dimensional visualization of the raw AE signals [16,17].

This study investigates the AE feature extraction and classification methodology for rail crack monitoring in the field typically with complex crack conditions and high operational noise. A series of field and laboratory tests were carried out to obtain the three types of AE waves, respectively induced by operational noise, impact and crack propagation. WT was applied to represent the features of AE waves in the time-frequency domain. After that, a deep CNN with transfer learning was designed and trained using the WT plots, and applied to classify different mechanisms of AE waves.

METHODOLOGY

The rail crack monitoring methodology proposed in this study is based on WT and CNN, where WT is applied to represent the features of AE waves in the time-frequency domain, and a deep CNN is developed as the feature extractor and the classifier to automatically detect multiple types of AE waves generated in the railway field. The overview of the methodology is shown in Figure 1. Firstly, as the preprocessing, the WT plots of raw AE waves were calculated, and then resized and normalized to be RGB figures of the same pixels. Secondly, datasets are constructed to train and validate the CNN, of which the architecture is optimized and the hyper-parameters are determined. Thirdly, a new testing dataset is constructed and input to the trained CNN in order to evaluate the performance and accuracy of classification.

Wavelet transform

Crack-related AE waves exhibit significant non-stationarity and are easy to be overwhelmed by noise in the time domain. Wavelet analysis is a powerful tool that has been applied to characterize non-stationary signals in the time-frequency domain [18]. Continuous wavelet transform (CWT) is defined as the convolution of signal $x(t)$ to be analyzed and a series of wavelet functions that are simply dilated and translated from a unique admissible mother wavelet [19].

$$WT(a,b) = \frac{1}{\sqrt{a}} \int_{-\infty}^{\infty} x(t) \psi^{*}\left(\frac{t-b}{a}\right) dt \tag{1}$$

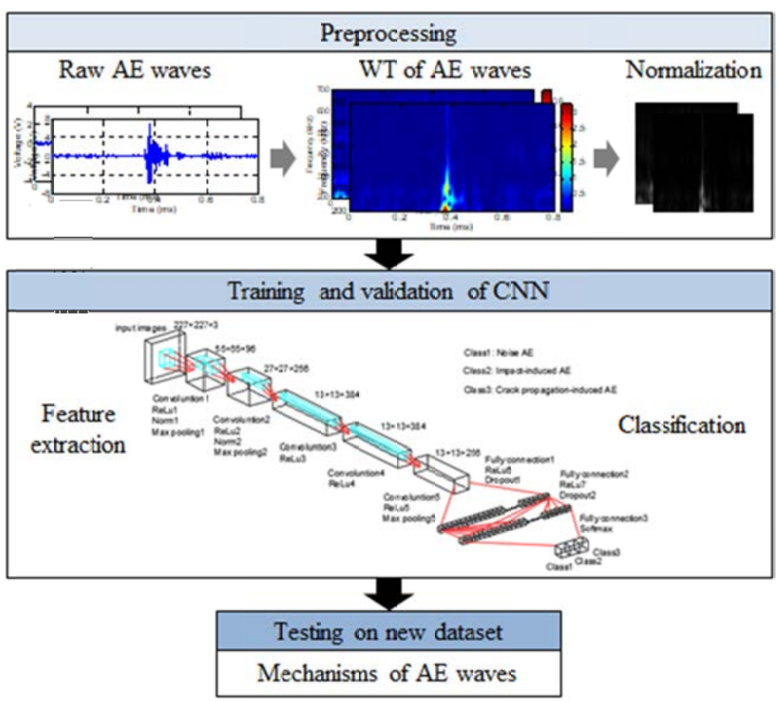

Figure 1. Schematic of the rail crack monitoring methodology.

Here, $a > 0$ is the scale parameter, b is the translation parameter, t is the time, and ψ^* denotes the complex conjugate of wavelet function ψ . $WT(a,b)$ is the matrix of wavelet coefficients, and its local maxima are achieved at dominant instantaneous frequencies. The choice of mother wavelet has a significant influence on the results of wavelet analysis. According to the references [4,20], the optimal mother wavelet was selected to be a complex Morlet wavelet, which provides excellent resolution in both of the time and frequency domains.

Deep convolutional neural network

CNN is a particular type of feedforward neural network directly working on two-dimensional data and widely used for image classification and object detection. It can effectively capture the grid-like topology of images, and requires fewer computations by using the sparsely connected neurons and the pooling process. These aspects make CNNs an efficient image recognition method [13]. A deep CNN is defined when its architecture is composed of many layers. A number of deep CNN architectures have been developed and adapted to research and industrial fields. The AlexNet architecture was adopted in this study, which has eight main layers and totally twenty-five sub-layers [21]. As listed in Table 1, the AlexNet architecture comprises five convolution (Conv) layers, three max-pooling (Pool) layers, seven nonlinear activation layers using the rectified linear unit (ReLU) function, two local response normalization (LRN) layers, three fully connected (FC) layers, two dropout layers, one softmax layer, one input layer and one classification (CL) layer. In order to save time for training and to achieve a more robust network using limited AE data that are available in this study, a pre-trained AlexNet was used for transfer learning. The Bayesian optimization algorithm was applied to tune the hyper-parameters of the CNN. The input of the network was RGB images of 227×227×3 pixels, and the output was the three mechanisms of AE waves.

TABLE I. DETAILED ARCHITECTURE OF ALEXNET USED IN THIS STUDY

Type	**Image size**	**Kernel number**	**Kernel size**	**Stride**	**Padding**	**Activation**	**LRN**	**Dropout**
Input	227x227x3	-	-	-	-	-	-	-
Conv1	55x55x96	96	11x11x3	[4 4]	[0 0 0 0]	ReLU	Yes	-
Pool1	55x55x96	-	3x3	[2 2]	[0 0 0 0]	-	-	-
Conv2	27x27x256	256	5x5x48	[1 1]	[2 2 2 2]	ReLU	Yes	-
Pool2	27x27x256	-	3x3	[2 2]	[0 0 0 0]	-	-	-
Conv3	13x13x384	384	3x3x256	[1 1]	[1 1 1 1]	ReLU	-	-
Conv4	13x13x384	384	3x3x192	[1 1]	[1 1 1 1]	ReLU	-	-
Conv5	13x13x256	256	3x3x192	[1 1]	[1 1 1 1]	ReLU	-	-
Pool5	13x13x256		3x3	[2 2]	[0 0 0 0]	-	-	-
FC6	4096	-	-	-	-	ReLU	-	Yes
FC7	4096	-	-	-	-	ReLU	-	Yes
FC8	1000	-	-	-	-	-	-	-
Softmax	3	-	-	-	-	-	-	-
CL	3	-	-	-	-	-	-	-

EXPERIMENTAL PROCEDURE

The AE data used in this study were collected through a series of field and laboratory tests. Field tests were carried out on a rail track with fatigue cracks and high operational noise. The details of the experimental setup can be found in the reference [6]. An incipient rolling contact fatigue crack with length less than 40 mm and depth less than 2 mm was focused in this study. There were passenger trains (axial load of about 17,000 kg and speed of about 120 km/h) and freight trains (axial load of about 21,000 kg and speed of about 80 km/h) operating on the rail track. AE data were collected when both types of trains passed by and generate various levels of rolling noise in order to realize a robust crack detection methodology. AE sensors were attached on both cracked and intact rails to obtain three typical types of AE waves encountered in the rail field.

The field crack propagated very slowly and the induced AE waves were mixed with other types of AE waves. It was difficult to collect and label enough crack propagation-induced AE waves in the field data for training the CNN. Three-point bending fatigue tests were thus carried out on rail steel specimens of different groove depths and peak loads to obtain more crack propagation-induced AE waves generated under various stress levels and load ratios. The details of the experimental setup can be found in the reference [4]. The crack propagation-induced AE waves used in this study were collected during the top 5% of load ranges.

AE data were acquired by a multi-channel AE system supplied by Physical Acoustics. The sensors used had a flat frequency response over the wide operating bandwidth of 125-1000 kHz, allowing more accurate study of the natural frequency characteristics of AE data. They were attached to the structural surface using adhesive couplant and fixed in place with magnetic clamps. The preamplifier gain was 40 dB and the sampling rate was 5 MHz. An analog band-pass filter of 100-1000 kHz was applied.

RESULTS AND DISCUSSION

There were totally 350 AE waves induced by operational noise and 350 AE waves induced by impact collected through the field tests, and 140 AE waves induced by propagation acquired through both of the field and laboratory tests. As the preprocessing, the WT plots of raw AE waves were calculated. According to reference [6], only the WT coefficients in frequency range of [200-700] kHz were of interest. Figure 2 displays nine examples of AE waves induced by the three mechanisms respectively. The maximum amplitudes of AE waves induced by both of crack propagation and impact were found to vary from 1 to 10 V, which overlapped with that of rolling noise. It is therefore necessary to present the AE waves in the time-frequency domain. As can be seen from the WT plots, the dominant frequency components of AE waves induced by rolling noise and impact were mainly below 300 kHz, and those of AE waves induced by crack propagation spread to 700 kHz. The three types of AE waves had different patterns in WT plots. However, it was difficult to make a simple index or criterion to classify them.

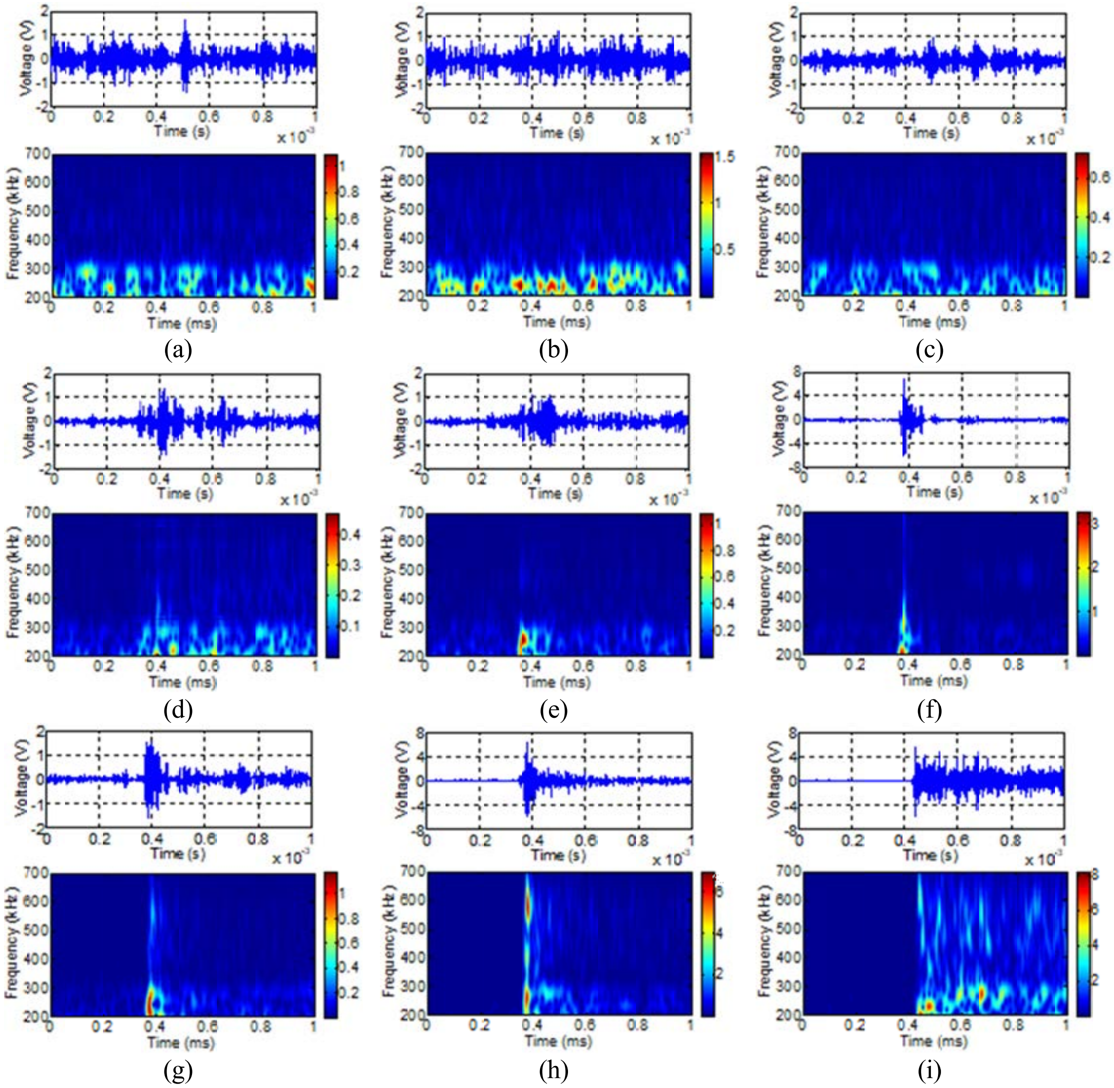

Figure 2. AE waves and their WT plots: (a)-(c) induced by noise, (d)-(e) induced by impact, and (g)-(i) induced by crack propagation.

The CNN was then applied to automatically learn features of the WT plots and classify them into three types corresponding to different mechanisms. 80% and 10% of the AE waves (i.e. totally 672 and 84 samples of the three types) were randomly chosen and used respectively for training and validation of the CNN with the proposed architecture. The reset 10% of AE waves (i.e. totally 84 AE samples of the three types) were used to test the performance of the trained CNN. By introducing the Bayesian optimization algorithm, the hyper-parameters of the CNN are tuned. The batch size is determined to be 50, the number of epochs is 58, and the learning rate is 0.00264. Figure 3 presents the training and validation accuracy as the number of iterations increased. The accuracy of validation dataset achieved 97.3%. For the testing dataset that had not been used for either training or validation, the classification accuracy achieved 97.6%. Figure 4 shows the confusion matrix of classification results for the testing dataset. As can be seen, all the noise-induced AE waves were labeled correctly, 2.9% of impact-induced AE waves were wrongly identified to be noise-induced ones, and 7.1% of crack propagation-induced AE waves were wrongly identified to be impact-induced ones.

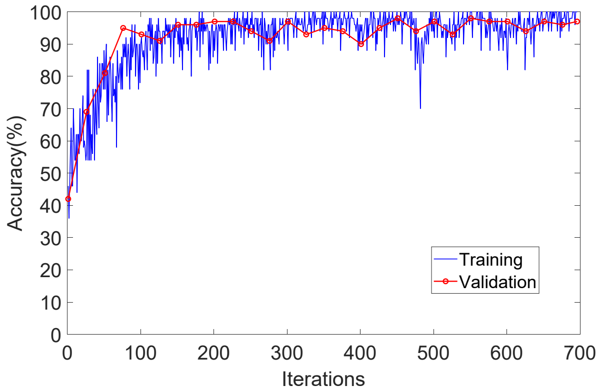

Figure 3. Accuracy versus the number of iterations during training and validation.

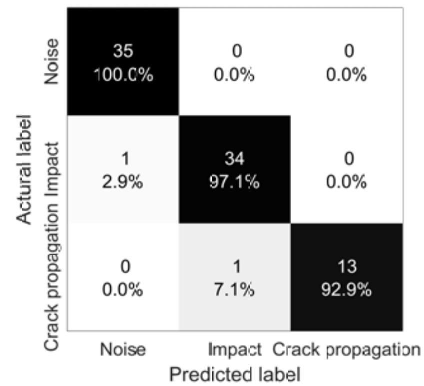

Figure 4. The confusion matrix of classification results for testing data.

CONCLUSIONS

The AE feature extraction and classification methodology was investigated in this study for rail crack monitoring in the railway field typically with complex crack conditions and high operational noise. The three types of AE waves respectively induced by operational noise, crack propagation and impact, were found to contain various instantaneous frequency components as represented in the WT plots. A deep convolutional neural network (CNN) with transfer learning was proposed to automatically extract features of the WT plots and classify the AE waves. The AlexNet architecture was adopted, and the hyper-parameters of the CNN were determined through Bayesian optimization. After training and validation using data collected through field and laboratory tests, the classification accuracy of testing dataset achieved 97.6%. The proposed methodology performed well in identifying different mechanisms of AE waves related to rail cracks. It should be noted that the proposed methodology is able to detect not only surface rail cracks where both impact-induced and crack propagation-induced AE waves could be observed, but also internal rail cracks where only crack propagation-induced AE waves could be observed.

ACKNOWLEDGEMENTS

Financial support from the National Natural Science Foundation of China (No. 51708164), the China Postdoctoral Science Foundation (No. 2018M632523) and the Fundamental Research Funds for the Central Universities in China (No. JZ2017HGBZ0954 and No. JZ2019HGTB0083) are acknowledged.

REFERENCES

1. Esveld, C. 2001. *Modern Railway Track. 2nd ed*. Zaltbommel: MRT-Productions.
2. Papaelias, M.P., Roberts, C. and Davis, C.L. 2008. "A review on non-destructive evaluation of rails: state-of-the-art and future development," *P. I. Mech. Eng. F.-J. Rai.*, 222(4): 367-384.
3. Ono, K. 2007. "Structural integrity evaluation using acoustic emission," *J. A. E.*, 25: 1-20.
4. Li, D., Kuang, K.S.C. and Koh, C.G. 2017. "Fatigue crack sizing in rail steel using crack closure-induced acoustic emission waves," *Meas. Sci. Technol.*, 28(6): 065601.

5. Thakkar, N.A., Steel, J.A. and Reuben, R.L. 2010. "Rail-wheel interaction monitoring using Acoustic Emission: a laboratory study of normal rolling signals with natural rail defects," *Mech. Syst. Signal Pr.*, 24(1): 256-266.
6. Li, D., Kuang, K.S.C. and Koh, C.G. 2018. "Rail crack monitoring based on Tsallis synchrosqueezed wavelet entropy of acoustic emission signals: A field study," *Struct. Health Monit.*, 17(6): 1410-1424.
7. Wang, J.F., Liu, X.Z. and Ni, Y.Q. 2018. "A Bayesian probabilistic approach for acoustic emission-based rail condition assessment," *Comput.-Aided Civ. Inf.*, 33(1): 21-34.
8. Pandya, D.H., Upadhyay, S.H. and Harsha, S.P. 2013. "Fault diagnosis of rolling element bearing with intrinsic mode function of acoustic emission data using APF-KNN," *Expert Syst. Appl.*, 40(10): 4137-4145.
9. Al-Dossary, S., Hamzah, R. and Mba, D. 2009. "Observations of changes in acoustic emission waveform for varying seeded defect sizes in a rolling element bearing," *Appl. Acoust.*, 70(1): 58-81.
10. Piotrkowski, R., Castro, E. and Gallego, A. 2009. "Wavelet power, entropy and bispectrum applied to AE signals for damage identification and evaluation of corroded galvanized steel," *Mech. Syst. Signal Pr.*, 23(2): 432-445.
11. Liu, Z., Han, Z., Zhang, Y. and Zhang, Q. 2014. "Multiwavelet packet entropy and its application in transmission line fault recognition and classification," *IEEE T. Neur. Net. Lear.*, 25(11): 2043-2052.
12. Marec, A., Thomas, J.H. and El Guerjouma, R. 2008. "Damage characterization of polymer-based composite materials: Multivariable analysis and wavelet transform for clustering acoustic emission data," *Mech. Syst. Signal Pr.*, 22(6): 1441-1464.
13. LeCun, Y., Bengio, Y. and Hinton, G. 2015. "Deep learning," *Nature*, 521: 436-444.
14. Cha, Y.-J., Choi, W. and Büyüköztürk, O. 2017. "Deep learning-based crack damage detection using convolutional neural networks," *Comput.-Aided Civ. Inf.*, 32(5): 361-378.
15. Xu, Y., Bao, Y., Chen, J., Zuo, W. and Li, H. "Surface fatigue crack identification in steel box girder of bridges by a deep fusion convolutional neural network based on consumer-grade camera images," *Struct. Health Monit.*, 18(3): 653-674.
16. Han, Y., Tang, B. and Deng, L. 2018. "Multi-level wavelet packet fusion in dynamic ensemble convolutional neural network for fault diagnosis," *Measurement*, 127: 246-255.
17. Islam, M.M.M. and Kim, J.-M. 2019. "Automated bearing fault diagnosis scheme using 2D representation of wavelet packet transform and deep convolutional neural network," *Comput. Ind.*, 106: 142-153.
18. Hamstad, M.A. and Gary, J. 2002. "A wavelet transform applied to acoustic emission signals: Part 1: Source identification," *J. A. E.*, 20: 39-61.
19. Teolis, A. 1998. *Computational Signal Processing with Wavelets*. Boston: Birkhäuser.
20. Ciampa, F. and Meo, M. 2010. "Acoustic emission source localization and velocity determination of the fundamental mode A0 using wavelet analysis and a Newton-based optimization technique," *Smart Mater. Struct.*, 19(4): 045027.
21. Krizhevsky, A., Sutskever, I. and Hinton, G.E. 2012. "Imagenet classification with deep convolutional neural networks," In *Advances in neural information processing systems*: 1097-1105.